eNeuro

Research Article: New Research

Novel Tools and Methods

Behavioral and Functional Brain Activity Alterations Induced by TMS Coils with Different Spatial Distributions

Gaby S. Pell,[1,2] Yiftach Roth,[1,2] Hamutal Shachar,[1,2] Moshe Isserles,[3] Noam Barnea-Ygael,[2] and Abraham Zangen[2]

https://doi.org/10.1523/ENEURO.0287-22.2023

[1]Department of Life Sciences and the Zlotowski Centre for Neuroscience, Ben-Gurion University of the Negev, Beer-Sheva, 84105, Israel, [2]BrainsWay Ltd., Jerusalem 9777518, Israel, and [3]Department of Psychiatry, Hadassah-Hebrew University Medical Center, Jerusalem, 91120, Israel

Abstract

Previous investigation of cognitive processes using transcranial magnetic stimulation (TMS) have explored the response to different stimulation parameters such as frequency and coil location. In this study, we attempt to add another parameter by exploiting the spatial profiles of TMS coils to infer regional information concerning reward-related behavior. We used different TMS coils to modulate activity in the prefrontal cortex (PFC) and examined resulting changes in behavior and associated brain activity. More specifically, we used the Figure-8 coil to stimulate a portion of the dorsolateral PFC (DLPFC) and the H-Coil to stimulate a larger volume within the lateral PFC (LPFC). Healthy human volunteers completed behavioral questionnaires ($n = 29$) or performed a reward-related decision-making functional MRI (fMRI) task ($n = 21$) immediately before and after acute high-frequency stimulation (10 Hz) with either a Figure-8 coil, H-Coil, or a sham coil. Stimulation was found to induce behavioral changes as well as changes in brain activation in key nodes of the reward network. Right LPFC, but not right DLPFC or sham, stimulation was found to induce changes in both behavioral scores and brain activation in key nodes of the reward system. In conclusion, this study supports the role of the right LPFC in reward-related behavior and suggest that the pathways through which the observed effects were generated are located outside the area of the DLPFC that is traditionally targeted with TMS. These results demonstrate the use of TMS coils with different spatial profiles as an informative tool to investigate anatomic and functional correlates of behavior.

Key words: electric fields; fMRI; neurostimulation; prefrontal cortex; reward; transcranial magnetic stimulation

Significance Statement

When trying to associate cognitive function with brain anatomy, probing with neuromodulation has emerged as a useful approach. One can modulate brain activity with techniques such as transcranial magnetic stimulation (TMS) and examine the effect on behavior. Yet, hypotheses often associate behavior with relatively large brain areas which is inefficient, requiring many experimental groups to provide useful information. Here, we describe an approach using TMS coils with different field distributions to achieve a similar goal with reduced time and simplified resources. Our results indicated a pattern that differed between a focal coil (Figure-8) coil and a wider/deeper coil (H-Coil). Future studies may localize the origin within the frontal cortex that drives these effects, and thereby further establish the association between structure and function.

Received July 17, 2022; accepted February 20, 2023; First published March 17, 2023.

A.Z. and Y.R. are inventors of the deep transcranial magnetic stimulation (DTMS) coil systems, serve as consultant and chief engineer (respectively) for, and has financial interests in BrainsWay. G.S.P. and H.M. have financial interest in BrainsWay.

Author contributions: A.Z., Y.R., H.S., and M.I. designed research; G.S.P., H.S., M.I., and N.B.-Y. performed research; G.S.P., A.Z., H.S., M.I., and N.B.-Y. analyzed data; G.S.P. and N.B.-Y. wrote the paper.

BrainsWay partially supported the study.

Acknowledgments: The authors wish to acknowledge and thank Dr. Yuval Porat and Andrei Averkin for their assistance during this study.

Introduction

A consistent finding across imaging studies of value-based learning and decision-making is the prominent involvement of the lateral prefrontal cortex (LPFC; Dixon and Christoff, 2014). Indeed, the LPFC, and especially the dorsolateral PFC (DLPFC) have been implicated in the pathogenesis of several psychiatric and neurologic disorders with affected reward-related behavior, including schizophrenia, anxiety, and posttraumatic stress disorder (Hopper et al., 2008; Maresh et al., 2014; Subramaniam et al., 2015; Park et al., 2016; Pu et al., 2016; Zhang et al., 2016). Moreover, there is evidence for the efficacy of transcranial magnetic stimulation (TMS) over the PFC for the treatment of other conditions with impaired reward-related behavior such as depression, addictions, Alzheimer's disease, schizophrenia, and eating disorders (Fox et al., 2014; Moeller et al., 2022). These effects are attributed to the technique's ability to redress imbalances in the excitability of brain networks and neurotransmitter concentrations that characterize these conditions (Pell et al., 2011). Notably, the United States Food and Drug Administration (FDA) has approved the use of TMS over the DLPFC for the treatment of major depression, a disorder in which anhedonia, believed to result from impaired processing in the brain's reward system, is a hallmark feature (APA, 2013). In fact, FDA approval has been given to two different classes of TMS coils, the Figure-8 and the H-Coil, following two multicenter trials (O'Reardon et al., 2007; Levkovitz et al., 2015). While the former generates a relatively superficial and focal effective electric field, the later induces a deeper and more widespread field (Roth et al., 2007; Rosenberg et al., 2010; Deng et al., 2013; Alyagon et al., 2020; Zibman et al., 2021). The differences in the depth-focality trade-off between the coils translate to a different volume of tissue being stimulated under each coil.

While the aforementioned effects of TMS were achieved in pathologic populations following repeated sessions, several studies have shown that acute TMS, when applied over the PFC of healthy individuals, affects specific reward-related behaviors (Levasseur-Moreau and Fecteau, 2012; Cho et al., 2015). A frequency dependence for this effect has been reported so while acute high-frequency stimulation over the left DLPFC increases responsiveness to rewarding stimuli in healthy subjects (Ahn et al., 2013), low-frequency stimulation over the right DLPFC lead to riskier decision-making (Knoch et al., 2006; Ahn et al., 2013). These observations complement previous investigations of cognitive processes using TMS, which have employed a variety of different stimulation parameters such as frequency, coil location, and dosage (Beynel et al., 2019).

A recent publication showed that rTMS with a focal Figure-8 coil differentially affects distinct clusters of symptoms in MDD patients depending on the placement of the coil (Siddiqi et al., 2020). While this finding is an important step in understanding the mechanism behind clinical rTMS, it also presents a tremendous challenge. Stimulating the target for each symptom cluster would require additional sessions to the current treatment protocol to treat each cluster in series. Alternatively, a larger coil that stimulates all cluster targets simultaneously was suggested by the authors to be more effective at poly-symptomatic treatment by uniformly modulating multiple clusters. They used clinical depression data from depression studies using the H-Coil and the Figure-8 to provide evidence for this claim.

Here, we set out to investigate whether the modified spatial distributions of the electric fields between the different coils can be further exploited to shed light on the localization of cognitive processes. More specifically, we used the Figure-8 coil to stimulate a portion of the DLPFC and the H-Coil to stimulate a larger volume within the LPFC. We hypothesized that coil-related differences will be evident both at a behavioral level and in the pattern of brain activity during reward-related tasks. To test this, a design was employed that separately examined functional and behavioral changes between measurements taken before (PRE) and immediately following (POST) acute stimulation. The novel study design offers the advantage of being able to relate findings back to the underlying anatomy and to shed light on regional specificity within the prefrontal cortex.

Materials and Methods

Procedure

The study design is summarized in Figure 1. The study included a feasibility component that aimed to determine the optimal choice of stimulation frequency (1 or 10 Hz) and location (left or right LPFC) for the effective induction of alterations in motivation. The main experiment employed the obtained parameters to investigate the neuronal correlates and behavioral consequences of alterations induced by acute stimulation with the different coils. This experiment included an functional MRI (fMRI) arm, in which subjects performed the Iowa Gambling Task (IGT) task inside the scanner, and a behavioral arm, in which questionnaire were completed to evaluate motivation [motivational VAS (mVAS); Stubbs et al., 2000; Gorwood et al., 2015], affect [positive and negative affect schedule (PANAS); Watson et al., 1988], or both [modified achievement goal questionnaire (AGQ); Elliot and Sheldon, 1997]. It should be noted that different sets of subjects were used in each stage of the experiment and for the behavioral and neuroimaging studies.

Subjects

TMS-naive volunteers ($n = 89$ participants; age: 24.2 ± 5.48 year; mean $\pm$ SD; 36 females) were recruited through advertising. All subjects were healthy with no history of psychiatric or neurologic diseases, and the different subgroups were stratified by age and gender using a computer program (Interactive Web Randomization System; Medpace's ClinTrak). Before participation, all subjects signed an

Correspondence should be addressed to Gaby S. Pell at mgpell@gmail.com.
https://doi.org/10.1523/ENEURO.0287-22.2023

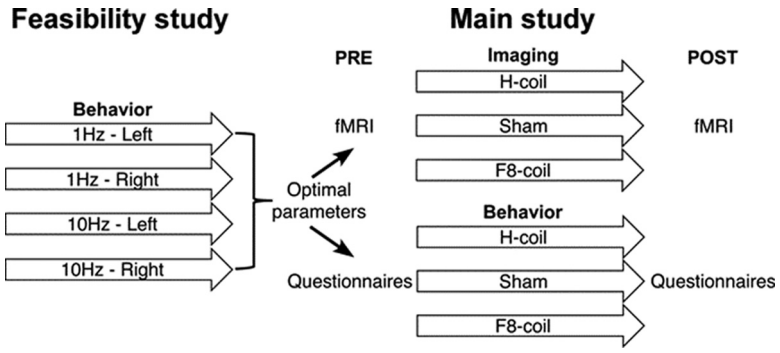

Figure 1. The study followed a two-stage trial design. The parameters for optimal induction of motivational alterations were determined in a feasibility study. These parameters were implemented in the imaging and behavioral parallel arms of the main study.

informed consent form and declared the absence of known TMS contraindications. Subjects were monetarily compensated ($30) for their time, and those who completed the fMRI decision-making task were given an additional payment according to their performance (up to $20). The study was approved by the local Institutional and National Review Board and was performed in accordance with the most recent version of the Declaration of Helsinki.

Transcranial magnetic stimulation

TMS was delivered with a Magstim Rapid^2 stimulator (Magstim) using three types of coils. The H6-coil (BrainsWay), designed according to the principles of deep TMS (Roth et al., 2002; Tendler et al., 2016; Alyagon et al., 2020) to convey a deep and widespread stimulation to the target area. The coil was air-cooled and was integrated within a helmet that attached firmly to the head. A sham TMS coil (BrainsWay), based on a toroidal winding, integrated within the same helmet as the H-Coil, which induced similar acoustic sensations but only negligible cortical electric field. An air-cooled Figure-8 coil (Magstim) that was attached to a standard gantry. A sketch of the coils and distribution maps of the induced electric fields are shown in Figure 2.

In accordance with the results of the feasibility trial, stimulation sessions consisted of high-frequency repetitive TMS (rTMS; 10 Hz, 2-s trains, 20-s intertrain interval) applied to the right PFC. In each session, 900 pulses were administered at an intensity of 120% of RMT, determined as the minimum stimulation output that induced 50% chance of visual thumb abduction (Pridmore et al., 1998). The target area, for all coils, was defined as the region 6 cm anterior to the primary motor hand area (M1; Herbsman et al., 2009; Johnson et al., 2013). Orientation of the Figure-8 coil was along the standard posterior-lateral direction (i.e., 45° with respect to the sagittal direction).

Sources of potential variability include subjective subject comfort during the stimulation, which may affect behavioral and functional MRI results. In order to compare this factor, subjects were asked to rate their overall feelings following the stimulation.

Neuroimaging

Stimulation-induced changes in neuronal activity were evaluated using a reward-related decision-making fMRI task [see below, Iowa Gambling Task (IGT)] that was executed PRE and POST stimulation with either the H-Coil, the Figure-8 coil, or the sham coil ($n = 21$ subjects, 7 in each group). To minimize the interval between the end of the stimulation session and the beginning of the second imaging session, the stimulation was performed in a room adjacent to the fMRI scanner and the subjects were returned to the scanner as quickly as possible after stimulation (<5 min).

Functional MRI

A Siemens 3T Trio MRI system (Siemens) was used together with a 32-channel RF coil. The parameters of the fMRI sequence were adjusted to minimize potential imaging artefacts in areas that were expected to be activated by the decision-making task (Deichmann et al., 2003). An initial pilot study was performed to determine the optimal parameters (data not shown). The following parameters were used for the gradient echoplanar imaging (EPI) BOLD sequence: TE = 25 ms, TR = 2000 ms, image matrix = 64 × 64, in-plane resolution = 3 × 3 mm, slice thickness = 3 mm with 1 mm gaps between slices, number of slices = 36, FOV = 192 mm, bandwidth = 220 kHz, volumes per scan = 405, duration of scan = 13.5 min. The slices were rotated from the transverse toward the coronal plane by 30° relative to the AC-PC line to reduce the influence of in-plane susceptibility gradients. The PRE scanning session comprised a localizer, a high-resolution anatomic scan (MP-RAGE sequence, TR/TE/TI = 8/4/1000 ms, image matrix = 256 × 256 × 70, resolution = 1 × 1×1 mm) and then the first functional run. The POST scanning session comprised a rapid localizer scan that was immediately followed by the second functional run.

Regions of interest (ROIs) were created in the targeted area ("target ROI") and in task-related areas ("task-related ROIs"). The target ROI was defined as the supra-threshold electrical field induced by the Figure-8 coil (Fig. 2), while the task-related ROIs selected major nodes of the reward network, the orbitofrontal cortex (OFC), anterior cingulate cortex (ACC), and the insular cortex (Bush et al., 2002; McClure et al., 2004; Haber, 2011; Albrecht et al., 2013). The pregenual ACC (pgACC) within Brodmann area 32 was selected as it has been strongly implicated in reward processing and subjective emotional state (Cho and Strafella, 2009; Dixon and Christoff, 2014). Brodmann area 11 was used to create an ROI in the OFC and

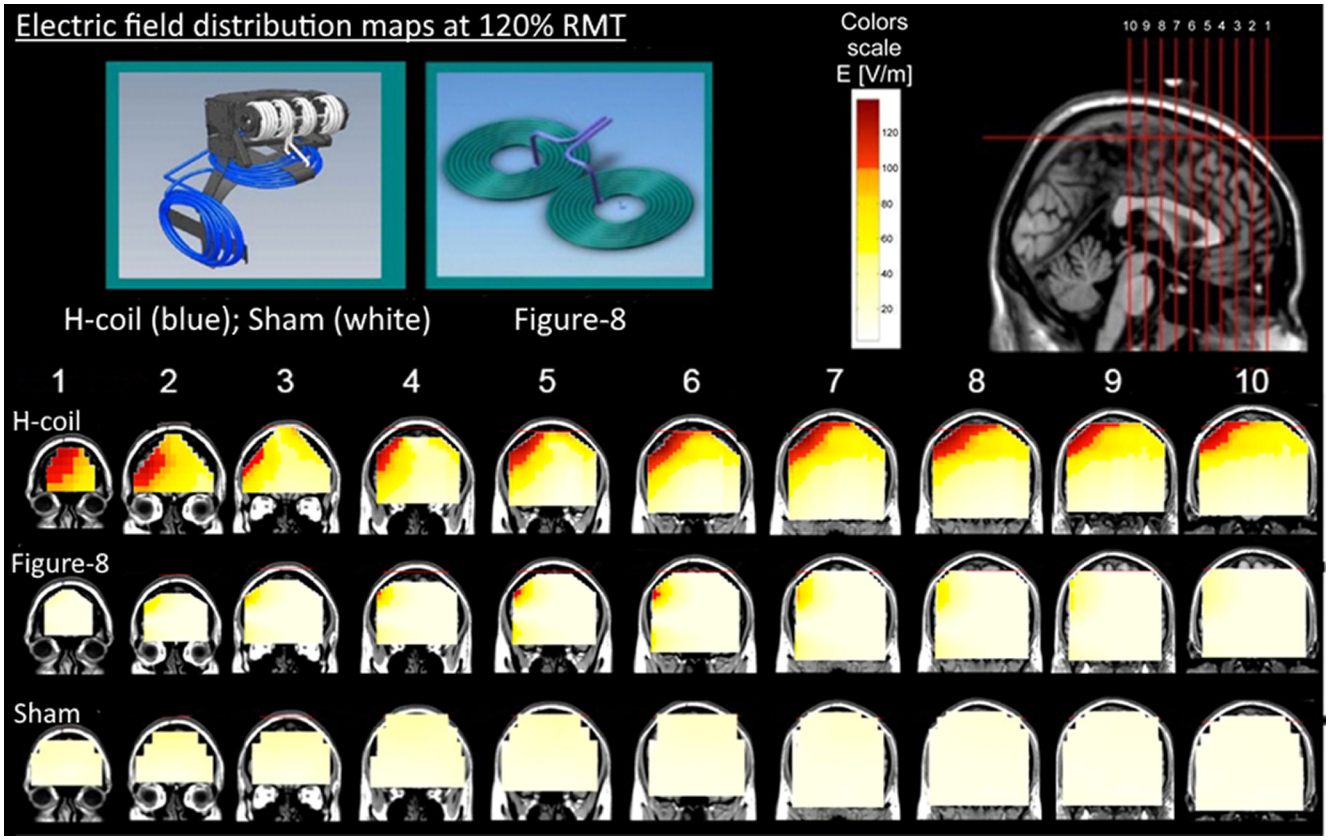

Figure 2. Electric field distributions induced by the TMS coils when placed over the right DLPFC, obtained in a phantom and overlaid on MRI images. The colored maps describe the absolute magnitude of the electric field for the various TMS coils. These were measured in a phantom model of the human head with an equivalent stimulation amplitude to that used in this study (i.e., stimulator output equivalent to 120% of an average motor threshold). In the color scale, red indicates a field magnitude above neural activation threshold (100 V/m), while white and yellow indicate field magnitude below the threshold. In the top left inset, the H-Coil is illustrated by the blue wire, while the sham coil is illustrated by the white wire wound on a cylindrical former. Anatomical images are shown in radiologic coordinates.

Brodmann area 13 was used to create an ROI in the insular cortex.

Iowa Gambling Task (IGT)

The subjects performed the task inside the scanner, PRE and POST stimulation. This probabilistic reward-related task was designed to be a simulation of real-life decision-making and was chosen for this study since it activates a wide range of brain areas involved with executive functions and reward-processing (Bechara et al., 2000; Li et al., 2010; Alexopoulos et al., 2015) that may overlap with the applied TMS field.

The goal of the task is to maximize profit. In brief, starting from an initial allocation of cards, subjects are required to make a series of card selections from one of four card decks (A, B, C, and D). Each selection is followed by the presentation of a reward and a penalty. Decks A and B are considered the disadvantageous decks because they yield high immediate rewards but higher long-term penalties and, consequently, a loss in the long-term. Decks C and D are the advantageous decks as they yield low immediate rewards but smaller long-term penalties, which, therefore, result in a long-term gain. The task was previously adapted for fMRI (Lin et al., 2008) and was programmed for the current study using the Presentation software package (Neurobehavioral Systems). The simple block design approach was selected to maximize the amplitude of the task-induced signal changes. The task comprised five blocks of the reward-based task interleaved with the same number of control (i.e., "rest") blocks. In the control task, the subjects were prompted to select the highest of four numbers presented instead of the cards. Each trial, consisting of one selection of four cards or numbers, lasted 4 s and each block consisted of 20 trials. Therefore, there was a total of 100 IGT trials in each scanning session. In the POST condition, the standard ABCD version of the task was substituted with a variant, known as EFGH, to minimize the learning effect (Bechara and Damasio, 2002; Bechara et al., 2002; Hernandez et al., 2006) and thus to reduce possible variation in brain activity between the PRE and POST conditions. The two versions differ with respect to the timing of losses and gains, so that while in the ABCD version gains are immediate and the losses are delayed, this situation is reversed for the EFGH variant. Subjects were told, before starting the EFGH task, that the strategy may differ to the previously completed task.

Table 1: Statistical table

Line	Analysis (variables)	Type of test	Statistic	*p*-value and confidence
	Stimulation			
a1	Subject comfort (H-Coil vs Figure-8)	Unpaired *t* test	$t = -0.58$; DoF = 26	$p = 0.56$; CI = (−1.61,0.89)
	fMRI (BOLD signal)			
a2	fMRI (time, coil) for target ROI	Two-way ANOVA	$F = 0.121$; DoF = (2,17)	$p = 0.9$
		Main effect TIME	$F = 0.04$; DoF = (1,17)	$p = 0.8$
		Main effect COIL	$F = 0.90$; DoF = (2,17)	$p = 0.4$
a3	fMRI (time, coil, ROI)	Three-way ANOVA	$F = 2.66$; DoF = (4,34)	$p = 0.49$; $\eta_p^2 = 0.25$
a4	fMRI (time, coil)	Two-way ANOVA	$F = 3.59$; DoF = (2,17)	$p = 0.50$; $\eta_p^2 = 0.30$
a5	*Post hoc* on *a4* (OFC)			
	H-Coil vs Figure-8	Simple main effect	Mean diff = 0.28	$p = 0.048^{\dagger}$; CI = (0.00,0.55)
	H-Coil vs sham	Simple main effect	Mean diff = 0.31	$p = 0.023^{\dagger}$; CI = (0.05,0.57)
a6	*Post hoc* on *a4* (pgACC)			
	H-Coil vs Figure-8	Simple main effect	Mean diff = 0.13	$p = 0.045^{\dagger}$; CI = (0.00,0.26)
	H-Coil vs sham	Simple main effect	Mean diff = 0.13	$p = 0.035^{\dagger}$; CI = (0.01,0.26)
a7	*Post hoc* on *a4* (insula)			
	H-Coil vs Figure-8	Simple main effect	Mean diff = 0.11	$p = 0.13^{\dagger}$; CI = (−0.06,0.42)
	H-Coil vs sham	Simple main effect	Mean diff = 0.11	$p = 0.26^{\dagger}$; CI = (−0.10,0.36)
	fMRI (task performance)			
a8	IGT behavior (coil, time)	Two-way ANOVA	$F = 0.86$; DoF = (2,17)	$p = 0.44$
	Behavior (coil)			
a9	mVAS (time, coil)	Two-way ANOVA	$F = 5.69$; DoF = (2,26)	$p = 0.009$; $\eta_p^2 = 0.3$
a10	*Post hoc* on *a9* (H-Coil)	Simple main effect	$F = 12.69$; DoF = (1,27)	$p = 0.001$; $r_2 = 0.4$
a11	ACQ (time, coil)	Two-way ANOVA	$F = 2.86$; DoF = (2,26)	$p = 0.076$; $\eta_p^2 = 0.18$
a12	*Post hoc* on *a11*	Main effect TIME	$F = 8.12$; DoF = (1,27)	$p = 0.01$
		Main effect COIL	$F = 0.11$; DoF = (2,27)	$p = 0.9$
a13	PANAS (time, coil)	Two-way ANOVA	$F = 0.28$; DoF = (2,26)	$p = 0.76$; $\eta_p^2 = 0.02$
	Extended material			
	fMRI per ROI (*post hoc*)			
a14	OFC (coil, time)	Two-way ANOVA	$F = 3.52$; DoF = (2,17)	$p = 0.048$; $\eta_p^2 = 0.30$
a15	pgACC (coil, time)	Two-way ANOVA	$F = 3.68$; DoF = (2,17)	$p = 0.047$; $\eta_p^2 = 0.31$
a16	Insular cortex (coil, time)	Two-way ANOVA	$F = 0.18$; DoF = (2,17)	$p = 0.18$; $\eta_p^2 = 0.18$
	Behavior (frequency, side)			
a17	VAS (side, frequency, time)	Three-way ANOVA	$F = 5.81$; DoF = (1,35)	$p = 0.021$; $\eta_p^2 = 0.15$
a18	VAS (frequency, time)	Two-way ANOVA	$F = 0.50$; DoF = (1,35)	$p = 0.04$; $\eta_p^2 = 0.01$
a19	VAS (side, time)	Two-way ANOVA	$F = 0.51$; DoF = (1,35)	$p = 0.51$; $\eta_p^2 = 0.01$
a20	*Post hoc* on *a19*, low frequency	Two-way simple-interaction	$F = 1.48$; DoF = (1,35)	$p = 0.23$; $r^2 = 0.04$
a21	*Post hoc* on *a19*, high frequency	Two-way simple-interaction	$F = 4.76$; DoF = (1,35)	$p = 0.01$; $r_2 = 0.12$
a22	*Post hoc* on *a19*, right LPFC	2nd order simple main effects	$F = 22.2$; DoF = (1,17)	$p = 0.001$; $r_2 = 0.56$
a23	ACQ (side, frequency, time)	Three-way ANOVA	$F = 0.12$; DoF = (1,35)	$p = 0.73$; $\eta_p^2 = 0.10$
a24	ACQ (frequency, time)	Two-way ANOVA	$F = 4.19$; DoF = (1,35)	$p = 0.048$; $\eta_p^2 = 0.11$
a25	ACQ (side, time)	Two-way ANOVA	$F = 1.27$; DoF = (1,35)	$p = 0.27$; $\eta_p^2 = 0.04$
a26	*Post hoc* on *a22*, high frequency	Simple main effect	$F = 12.2$; DoF = (1,17)	$p = 0.001$; $r^2 = 0.64$
a27	PANAS (side, frequency, time)	Three-way ANOVA	$F = 0.02$; DoF = (1,35)	$p = 0.90$; $\eta_p^2 = 0.00$
a28	PANAS (frequency, time)	Two-way ANOVA	$F = 1.90$; DoF = (1,35)	$p = 0.18$; $\eta_p^2 = 0.05$
a29	PANAS (side, time)	Two-way ANOVA	$F = 0.35$; DoF = (1,35)	$p = 0.56$; $\eta_p^2 = 0.00$

All data were checked for normal distribution (see Materials and Methods, Statistical data and analysis).
CI: confidence interval.
DoF: degrees of freedom.
IGT: Iowa Game Task.
mVAS, ACQ, PANAS: behavioral questionnaires.
OFC, pgACC, insular: regions of interest.
† uncorrected *p*-value (multiply *p*-value by three for Bonferroni correction).

Behavior

Subjects completed a battery of questionnaires both before and following stimulation with either the H-Coil, the Figure-8 coil, or the sham coil ($n = 9$, 8, and 12, respectively). The questionnaires were identical to those used in the feasibility study (see Extended Data Fig. 6-1 for a description). They included the mVAS questionnaire, which assesses motivation to undertake various actions (Stubbs et al., 2000; Gorwood et al., 2015); the AGQ, which evaluates two goal orientations toward a specific reward (Elliot and Sheldon, 1997); and the PANAS, which assesses emotional state (Watson et al.,

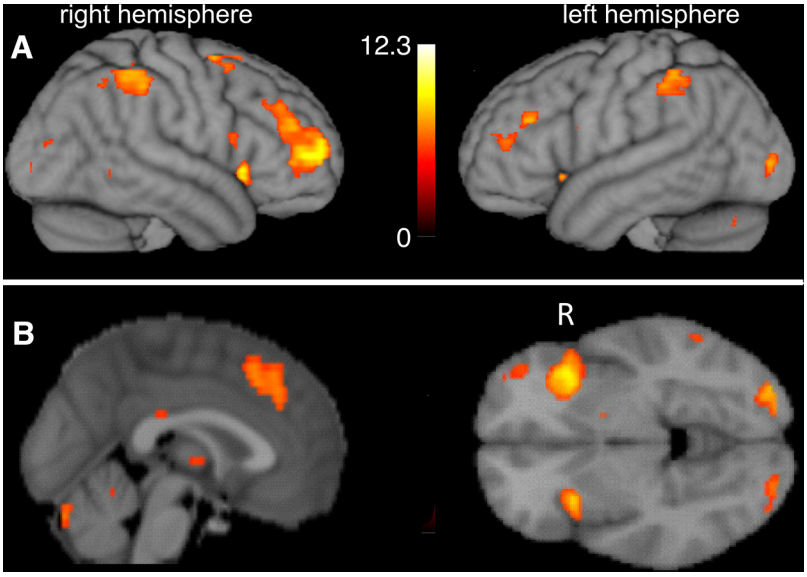

Figure 3. Group activation maps obtained while performing the IGT in the PRE (i.e., prestimulation) condition. Statistical maps (task > rest) are overlaid on a rendered cortical surface (***A***) or orthogonal slices (***B***) for a threshold of $p = 0.05$ with FWER correction. (L/R indicates left/right hemisphere in ***A*** and left/right sides of the image in ***B***, respectively.)

1988). Subjects were asked to answer the items in the questionnaires according to how they felt at that moment to prevent, to as great an extent as possible, any effects of expectation or learning in the POST condition. In addition, all questionnaires were administered in writing and subjects were told that the data would be anonymized, to reduce social bias. The questionnaires were always administered to the subjects in the same order (mVAS→AGQ→PANAS).

Statistics and data analysis

Neuroimaging

Image preprocessing and analysis were performed with the SPM8 software package (FIL), and the FSL package (fMRIB) was used for ROI drawing and data extraction.

The imaging data from each subject were first analyzed to identify areas of decreased and increased activation in the task blocks relative to the control ("rest") blocks. The modeled fMRI signal was convolved with the hemodynamic response function, and low-frequency noise was removed with a high-pass filter (cutoff = 165 s). Group activation during the PRE IGT session was thresholded at $p = 0.05$ with voxel-level correction for familywise error rate (FWER). In the next stage, ROIs were drawn in the preselected areas described above and applied to the SPM contrast images containing the contrast of the parameter estimates at each voxel (contrast: task > rest) that had been obtained at the first-level in the PRE and POST images. The subsequent mixed model factorial ANOVA analyses investigated (1) the target ROI with a model comprising the factors TIME (within-subjects, two levels: PRE, POST) and COIL (between-subjects, three levels: H-Coil, Figure-8 coil, and sham), or (2) the reward-related ROIs with a model comprising the factors TIME (within-subjects, two levels: PRE, POST), COIL (between-subjects, three levels: H-Coil, Figure-8 coil, and sham) and ROI (within subjects, three levels: pgACC, right OFC, right insula). In order to establish the basis of the factorial ANOVA analysis, differences in the baseline (PRE) data between the coil groups were analyzed with one-way ANOVA tests and the normality assumption was assessed (Kolmogorov–Smirnov test on the residuals).

Behavior

Analysis was conducted using the SPSS statistical package (SPSS v20, IBM). In order to establish the basis of the factorial ANOVA analysis, the data were evaluated for normality and homogeneity of variances. Group differences in the baseline (PRE) data were analyzed with *t* tests. Unless stated otherwise, all effects are reported as significant at $p \leq 0.05$. The effect of stimulation field distribution on the behavioral scores was analyzed with a two-way mixed 2×3 ANOVA design, with the factors TIME (PRE, POST) and COIL (H-Coil, Figure-8 coil, sham coil).

Decomposition of a significant interactions in factorial ANOVA analyses allows the origin of the finding to be explored in the framework of follow-up analyses. The approach of "simple effects" following significant findings and main effects following nonsignificant findings was employed (see Howell and Lacroix, 2012; their Fig. 1). Simple effects are commonly encountered in the form of simple main effects that are used to decompose a significant two-way interaction in which the effect of one independent variable is examined at individual levels of the other independent variable (Field, 2009). The equivalent approach following a significant three-way interaction is known as simple interaction effects (Howell and Lacroix, 2012). Effect sizes were calculated as partial η^2 (η_p^2) for the main factorial analyses and as correlation coefficients for the single main effects analyses.

Results

Establishment of TMS protocol

High frequency stimulation of the right hemisphere was selected in the feasibility stage of the study since it was found to induce a greater degree of modulation of reward-motivated performance, corresponding to a general decrease in the behavioral scores (see Extended Data Figs. 6-2, 6-3). All subjects tolerated the rTMS well, and no serious adverse events were observed or reported. In addition, there were no significant differences between H-Coil and Figure-8 coil groups in self-reported ratings of comfort during stimulation ($t_{(15)} = -0.58$, $p = 0.6$[a1]). All statistics are summarized in Table 1.

Average stimulus output intensities at threshold were $62 \pm 10\%$ and $68 \pm 8\%$ for the Figure-8 coil and H-Coil, respectively. Differences in the stimulation intensity at threshold are expected because of the different coil designs. However, it is important to note that by calibrating the rTMS stimulus intensity in the standard manner according to the subject's threshold, the study thereby is evaluating the effect of the different field distributions of the coils (Fig. 2) after fixing the strength of the electric field at the level of the hand motor cortex.

Neuroimaging

Subjects were stimulated with either the H-Coil, Figure-8 coil, or sham coil. The data of one subject from the Figure-8 coil group were excluded because of head motion exceeding 2 mm that was observed during preprocessing. No differences were observed between the groups with regards to IGT performances, at both the PRE and POST conditions.

The group activation map obtained during the PRE task from all the subjects (i.e., $n = 20$) is shown overlaid on the cortical surface and orthogonal slices (Fig. 3*A*,*B*). Areas commonly included in the task-positive network such as the DLPFC and insula are observed.

In the mixed model ANOVA, no statistical differences were observed in the baseline (i.e., PRE) data across the coil groups and normality of residuals was confirmed. In the analysis of the target ROI, no significant terms were found either in the interaction or main effects (TIME × COIL: $F_{(2,17)} = 0.121$, $p = 0.9$; TIME: $F_{(1,17)} = 0.04$, $p = 0.8$; COIL: $F_{(2,17)} = 0.90$, $p = 0.4$[a2]) indicating that the task did not differentially activate this region between the stimulation states. In the analysis of the task-related ROIs, the three-way interaction (TIME × COIL × ROI) was found to be significant ($F_{(4,34)} = 2.66$, $p = 0.049$, partial $\eta^2 = 0.25$[a3]) indicating two-way interactions that vary across levels of the third variable. The TIME × COIL term was also significant ($F_{(2,17)} = 3.59$, $p = 0.05$, partial $\eta^2 = 0.30$[a4]) which is suggestive of a consistent influence of the coil on the stimulation-induced activation regardless of the particular ROI. The plot of TIME × COIL interaction was visually characterized by opposing sign of the "slope" (i.e., POST-PRE activation-induced change) for the H-Coil stimulation group compared with the two other stimulation groups (Fig. 4*A*). Follow-up analysis of the TIME × COIL interaction plots at each level of ROI consistently indicated this same visual pattern of opposing slopes (see Fig. 4*B–D*). Evaluation of these simple main effects of the TIME × COIL term confirmed that in two of the three ROIs, the poststimulation activation for the H-Coil displayed a trend of difference relative the Figure-8 and sham coils (for example, in the right orbitofrontal cortex ROI, H-Coil vs Figure-8 mean difference $= 0.23 \pm 0.13$. $p_{uncorrected} = 0.045$; H-Coil vs sham mean difference $= 0.31 \pm 0.13$. $p_{uncorrected} = 0.05$[a5,a6,a7]).

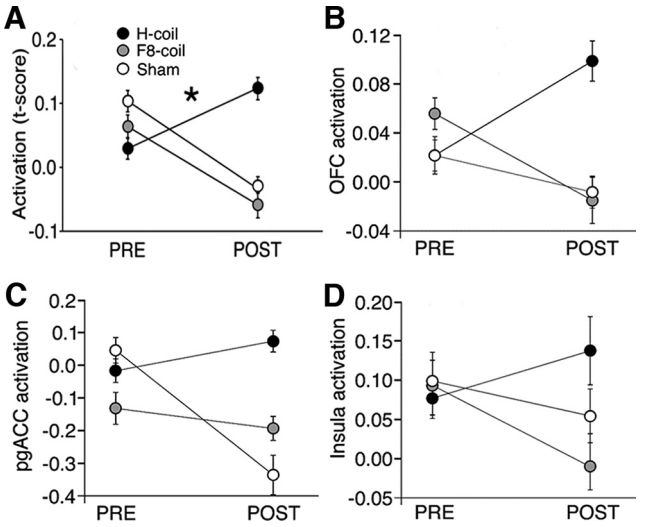

Figure 4. ***A***, Effect of stimulation group on functional activation from the significant interaction (TIME × COIL) from the complete factorial model (TIME × COIL × ROI). Activation, shown on the *y*-axis, is represented by the SPM contrast image for task > rest. The plots thereby indicate the stimulation-induced activation for the three stimulation groups over the two time points (PRE and POST) and the corresponding slopes characterize the sign of this activation-induced change. The ROIs were in areas of the putative reward network, in the right OFC, right insula, and pgACC. Extended Data Figure 4-1 in the extended material shows the corresponding plot for changes in the behavioral performance metric measured during the IGT task. ***B–D***, Exploratory analysis of TIME × COIL interaction in each of the individual ROIs, the right orbitofrontal cortex (***B***), the pregenual ACC (***C***), and the right insular cortex (***D***). The same pattern of opposing slopes shown in ***A*** is consistently observed in these individual ROIs that represented a non-significant trend following correction for multiple comparisons (right OFC ROI: $F_{(2,17)} = 3.52$, $p_{uncorrected} = 0.048$, $p_{corrected} = 0.14$, $\eta_p^2 = 0.30$[a13]; pgACC ROI: $F_{(2,17)} = 3.68$, $p_{uncorrected} = 0.047$, $p_{corrected} = 0.14$, $\eta_p^2 = 0.31$[a14]; right insular cortex: $F_{(2,17)} = 1.9$, $p_{uncorrected} = 0.18$, $p_{corrected} = 0.54$, $\eta_p^2 = 0.18$[a15]). Errors bars are ±SEM, * indicates a significant interaction ($p < 0.05$).

The behavioral performance metric measured during the IGT task did not significantly differ between stimulation groups ($F_{(2,17)} = 0.864$, $p = 0.44$[a7]; see Extended Data Fig. 4-1).

To further explore the spread of this signal pattern, a voxel-wise explorative analysis was conducted across the brain, to reveal areas in which this phenomenon of opposing activation-induced slope was observed even in the absence of a significant statistical interaction. The analysis found the pattern to be repeated in widespread areas of the brain, with a clear division along the anterior-posterior axis of the brain (Fig. 5). That is, anterior areas were largely characterized by a positive slope of activation-induced change (i.e., POST>PRE) following H-Coil

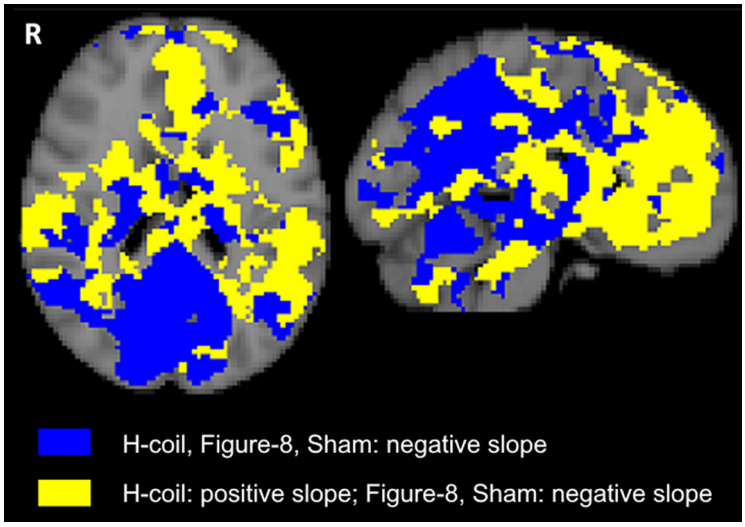

Figure 5. Explorative analysis showing intercoil pattern of slopes, defined as the change in the activation contrast of task > rest between the POST and PRE scans, i.e., as POST-PRE. Two representative orthogonal slices are shown with Talairach slice positions: axial (left): z = 20 cm; sagittal (right): x = −4 cm. Yellow voxels represent the stereotypical pattern of activation seen across the three selected ROIs in the reward system, i.e., with a positive slope in the H-Coil stimulation group and a negative slope in the Figure-8 coil and Sham stimulation groups. Blue voxels represent the nondifferential pattern of activation (namely, negative slopes for all stimulation groups).

stimulation and negative slope following Figure-8 coil or Sham stimulation, while posterior areas were largely characterized by negative slopes (i.e., PRE>POST) across all stimulation conditions.

Behavior

No statistical differences in the baseline (PRE) data between the coil groups were observed for any of the behavioral measures and normality of residuals was confirmed. Following high frequency stimulation of the right PFC, analysis of the mVAS scores revealed a significant TIME × COIL interaction ($F_{(2,26)} = 5.69$, $p = 0.009$, $\eta^2_p = 0.3$ [a8]; see Fig. 6*A*), and decomposition for simple main effects revealed significantly decreased score only following H-Coil stimulation ($F_{(1,27)} = 12.69$, $p = 0.001$, $r^2 = 0.4$[a9]), but not following Figure-8 coil or Sham stimulation, thereby indicating that it was the behavior of the H-Coil that drove the interaction. Analysis of the AQG scores indicated a similar qualitative pattern. In this case however, the TIME × COIL interaction did not reach significance ($F_{(2,27)} = 2.86$, $p = 0.076$, $\eta^2_p = 0.18$; Fig. 6*B*)[a10]. The main effect of TIME was significant ($F_{(1,27)} = 8.12$, $p = 0.01$), while the main effect of COIL was not significant ($F_{(2,27)} = 0.11$, $p > 0.05$)[a11]. Exploratory analysis of simple main effects again indicated significantly decreased score following H-Coil stimulation ($F_{(1,27)} = 12.21$, $p = 0.002$, $r^2 = 0.3$[a11]), but not following Figure-8 coil or Sham stimulation. Analysis of the PANAS scores revealed no significant interactions ($F_{(2,26)} = 0.28$, $p = 0.76$, $\eta^2_p = 0.02$[a12]) or simple main effects.

Discussion

This is the first study that compares patterns of activation that are generated following stimulation with the

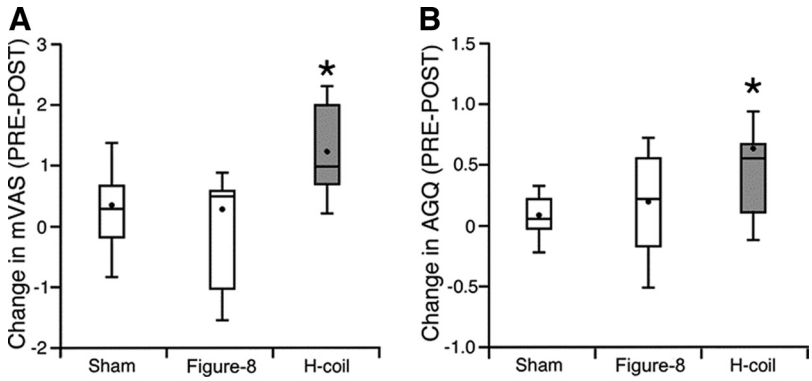

Figure 6. Behavioral changes in motivation induced by the various stimulation coils (defined as PRE-POST). In each box of the mVAS (***A***) and AGQ (***B***) scores as measured by the questionnaires, the horizontal band indicates the group median, the dot indicates the group mean, and the whiskers define the extent of 1.5 times the interquartile range. Extended Data Figure 6-1 in the Extended Data shows detailed explanations of the questionnaires. Extended Data Figures 6-2 and 6-3 show analyses of these measures obtained in the preliminary feasibility study. *$p < 0.05$ between PRE and POST H-Coil stimulation.

Figure-8 coil and the H-Coil. It was found that right-sided stimulation at high-frequency led to reduced behavioral scores and a unique pattern of activation changes following H-Coil, but not Figure-8 coil or Sham stimulation. Taken together with the more focal spatial distribution of the electric field induced by the Figure-8 coil and the lack of coil-related differences in the target ROI, these results suggest that the origin of the observed effects is outside the area in the DLPFC conventionally targeted during TMS treatment, but inside the wider stimulation area of the H-Coil. Future experiments may identify an exact location in the wider LPFC, or even in more remote areas such as the medial PFC. Alternatively, it is possible that the effect is generated in deeper layers of the DLPFC that are beyond the reach of the Figure-8 coil.

While the study has demonstrated the ability of TMS to modulate motivational behavior, the reduction in these measures observed with stimulation in the chosen PFC target is evidence of the complex relationship of brain stimulation and cognitive function where "improvements" in function are often hard to achieve because of the complex brain networks involved (Sack and Linden, 2003).

The feasibility stage of the study selected high frequency stimulation of the right hemisphere as it was found to induce a greater degree of modulation of reward-motivated performance. Interestingly, this was found to be the optimal protocol for treatment of attention-deficit disorder (ADHD) using the same coil, presumably because of its ability to effectively reduce response inhibition and reward-based decision-making (Alyagon et al., 2020). Left-sided stimulation surprisingly did not induce a corresponding increase in performance which might reflect the difficulty in inducing such a change in healthy subjects. The decrease in motivation, as assessed by the mVAS and AGQ questionnaires, following right-sided stimulation appears to be in accordance with the theory of hemispheric specialization of the PFC (Davidson, 1992; Heller et al., 1995; Coan and Allen, 2004; Pizzagalli et al., 2005; Spielberg et al., 2012) and the rationale for DLPFC stimulation for the treatment of depression. That is, while high-frequency stimulation of the left DLPFC is expected to alleviate the anhedonic and amotivational symptoms of depression, stimulation of its contralateral homolog is expected to do the opposite. In our healthy volunteers, where the hedonic and motivational states are not compromised, a ceiling effect may have prevented additional improvement following left stimulation, but impaired motivation following right stimulation.

The effect of stimulation on reward-related behavior was significant only for the more widespread stimulation with the H-Coil. This may follow the simple consequence that coils with a broader field profile will be more likely to overlap with the location of the optimal target region; alternatively, stimulation of multiple, deeper or more downstream targets, may also play a role. For example, connectivity-based targeting (Fox et al., 2012) showed that the efficiency of rTMS treatment of depression is related to the strength of the connectivity between the stimulated region within the DLPFC and the subgenual ACC (sgACC), a deep brain structure which has an important role in the reward circuitry.

While the Figure-8 coil and Sham stimulation did not affect motivational behavior performance, the H-Coil lead to reduced score in the "pure" motivational questionnaire (mVAS), intermediate reduction of scores in the questionnaire that combine motivational and affective influences (AGQ) and did not affected scores in the "pure" affective questionnaire (PANAS). These results suggest that H-Coil stimulation influenced the cognitive, rather than the affective, aspects of goal-oriented behavior, a result that is line with former publications (Jenkins et al., 2002; Levkovitz et al., 2007). However, an alternative interpretation is that the effect of stimulation decayed faster than expected, and the degree of influence over the different questionnaires is because of the order of their administration (i.e., mVAS→AGQ→PANAS).

The neuroimaging data confirmed the influence of the spatial field distribution by showing that stimulation-induced change in fMRI activation across several regions in the reward network displayed a unique behavior in the group that received stimulation with the H-Coil. This corresponded to the observation of a characteristic pattern in the plots of PRE versus POST activation. On further examination, this pattern was predominantly in anterior areas of the brain, within areas commonly associated with both the Task Negative network (e.g., dACC and ventromedial PFC) and the Task Positive network (e.g., insula and ventrolateral PFC).

A recent study by Siddiqi et al. (2020), showing that focal TMS affects distinct aspects of MDD symptoms depending on coil location, suggests the utilization of coils with less focality to potentially provide symptom-wide benefits. Our study has shown that combinations of coils with different spatial characteristics can be used to aid our understanding of the anatomic origin of complex cognitive and behavioral processes.

We acknowledge several limitations to this study, principally the relatively small sample sizes. While the hypothesis-driven imaging analysis was restricted to ROIs in the reward system, a data-driven whole-brain voxel-wise analysis revealed a pattern of signal changes that was replicated across widespread areas of the brain. However, discussion related to the nonsignificant findings is speculative. Finally, it should be noted that neuro-navigation was not used in this study, which may have influenced the results of focal stimulation.

In conclusion, this study used distinct stimulation profiles of TMS coils to investigate the manipulation of reward-related behavior and neuronal function. This approach was shown to represent a promising tool to explore the regional specificity of behavior. The study thus supports the use of different TMS coil types and TMS targets to enhance our understanding of human behavior. These findings contribute to the growing knowledge of the neurobiology of cognition and may provide the basis of innovative protocols for the controllable modulation of reward-oriented behavior.

References

Ahn HM, Kim SE, Kim SH (2013) The effects of high-frequency rTMS over the left dorsolateral prefrontal cortex on reward responsiveness. Brain Stimul 6:310–314.

Alexopoulos GS, Manning K, Kanellopoulos D, McGovern A, Seirup JK, Banerjee S, Gunning F (2015) Cognitive control, reward-related decision making and outcomes of late-life depression treated with an antidepressant. Psychol Med 45:3111–3120.

Alyagon U, Shahar H, Hadar A, Barnae-Ygael N, Lazarovits A, Shalev H, Zangen A (2020) Alleviation of ADHD symptoms by non-invasive right prefrontal stimulation is correlated with EEG activity. Neuroimage Clin 26:102206.

Albrecht K, Volz KG, Sutter M, von Cramon DY (2013) What do I want and when do I want it: brain correlates of decisions made for self and other. PLoS One 8:e73531.

APA (2013) American Psychiatric Association, diagnostic and statistical manual of mental disorders, Ed 5. Washington, DC: American Psychiatric Publishing.

Bechara A, Damasio H (2002) Decision-making and addiction (part I): impaired activation of somatic states in substance dependent individuals when pondering decisions with negative future consequences. Neuropsychologia 40:1675–1689.

Bechara A, Tranel D, Damasio H (2000) Characterization of the decision-making deficit of patients with ventromedial prefrontal cortex lesions. Brain 123:2189–2202.

Bechara A, Dolan S, Hindes A (2002) Decision-making and addiction (part II): myopia for the future or hypersensitivity to reward? Neuropsychologia 40:1690–1705.

Beynel L, Appelbaum LG, Luber B, Crowell CA, Hilbig SA, Lim W, Nguyen D, Chrapliwy NA, Davis SW, Cabeza R, Lisanby SA, Deng Z (2019) Effects of online repetitive transcranial magnetic stimulation (rTMS) on cognitive processing: a meta-analysis and recommendations for future studies. Neurosci Biobehav Rev 107:47–58.

Bush G, Vogt BA, Holmes J, Dale AM, Greve D, Jenike MA, Rosen BR (2002) Dorsal anterior cingulate cortex: a role in reward-based decision making. Proc Natl Acad Sci U S A 99:523–528.

Cho SS, Strafella AP (2009) rTMS of the left dorsolateral prefrontal cortex modulates dopamine release in the ipsilateral anterior cingulate cortex and orbitofrontal cortex. PLoS One 4:e6725.

Cho SS, Koshimori Y, Aminian K, Obeso I, Rusjan P, Lang AE, Daskalakis ZJ, Houle S, Strafella AP (2015) Investing in the future: stimulation of the medial prefrontal cortex reduces discounting of delayed rewards. Neuropsychopharmacology 40:546–553.

Coan JA, Allen JJ (2004) Frontal EEG asymmetry as a moderator and mediator of emotion. Biol Psychol 67:7–49.

Davidson RJ (1992) Anterior cerebral asymmetry and the nature of emotion. Brain Cogn 20:125–151.

Deichmann R, Gottfried JA, Hutton C, Turner R (2003) Optimized EPI for fMRI studies of the orbitofrontal cortex. Neuroimage 19:430–441.

Deng ZD, Lisanby SH, Peterchev AV (2013) Electric field depth–focality tradeoff in transcranial magnetic stimulation: simulation comparison of 50 coil designs. Brain Stimul 6:1–13.

Dixon ML, Christoff K (2014) The lateral prefrontal cortex and complex value-based learning and decision making. Neurosci Biobehav Rev 45:9–18.

Elliot AJ, Sheldon KM (1997) Avoidance achievement motivation: a personal goals analysis. J Pers Soc Psychol 73:171–185.

Field A (2009) Discovering statistics using SPSS. Thousand Oaks: SAGE Publications.

Fox MD, Buckner RL, White MP, Greicius MD, Pascual-Leone A (2012) Efficacy of transcranial magnetic stimulation targets for depression is related to intrinsic functional connectivity with the subgenual cingulate. Biol Psychiatry 72:595–603.

Fox MD, Buckner RL, Liu H, Chakravarty MM, Lozano AM, Pascual-Leone A (2014) Resting-state networks link invasive and noninvasive brain stimulation across diverse psychiatric and neurological diseases. Proc Natl Acad Sci U S A 111:E4367–E4375.

Gorwood P, Vaiva G, Corruble E, Llorca PM, Baylé FJ, Courtet P (2015) The ability of early changes in motivation to predict later antidepressant treatment response. Neuropsychiatr Dis Treat 11:2875–2882.

Haber SN (2011) Neuroanatomy of reward: a view from the ventral striatum. In: Neurobiology of sensation and reward, p 235. Boca Raton: CRC Press/Taylor & Francis.

Heller W, Etienne MA, Miller GA (1995) Patterns of perceptual asymmetry in depression and anxiety: implications for neuropsychological models of emotion and psychopathology. J Abnorm Psychol 104:327–333.

Herbsman T, Avery D, Ramsey D, Holtzheimer P, Wadjik C, Hardaway F, Haynor D, George MS, Nahas Z (2009) More lateral and anterior prefrontal coil location is associated with better repetitive transcranial magnetic stimulation antidepressant response. Biol Psychiatry 66:509–515.

Hernandez M, Lu X, Hyonggin A, Bechara A (2006) Development of parallel versions of the Iowa Gambling Task for repeat testing. J Int Neuropsych Soc 12:44.

Hopper JW, Pitman RK, Su Z, Heyman GM, Lasko NB, Macklin ML, Orr SP, Lukas SE, Elman I (2008) Probing reward function in post-traumatic stress disorder: expectancy and satisfaction with monetary gains and losses. J Psychiatr Res 42:802–807.

Howell GT, Lacroix GL (2012) Decomposing interactions using GLM in combination with the COMPARE, LMATRIX and MMATRIX subcommands in SPSS. TQMP 8:1–22.

Jenkins J, Shajahan PM, Lappin JM, Ebmeier KP (2002) Right and left prefrontal transcranial magnetic stimulation at 1 Hz does not affect mood in healthy volunteers. BMC Psychiatry 2:1.

Johnson KA, Baig M, Ramsey D, Lisanby SH, Avery D, McDonald WM, Li X, Bernhardt ER, Haynor DR, Holtzheimer PE 3rd, Sackeim HA, George MS, Nahas Z (2013) Prefrontal rTMS for treating depression: location and intensity results from the OPT-TMS multisite clinical trial. Brain Stimul 6:108–117.

Knoch D, Gianotti LR, Pascual-Leone A, Treyer V, Regard M, Hohmann M, Brugger P (2006) Disruption of right prefrontal cortex by low-frequency repetitive transcranial magnetic stimulation induces risk-taking behavior. J Neurosci 26:6469–6472.

Levasseur-Moreau J, Fecteau S (2012) Translational application of neuromodulation of decision-making. Brain Stimul 5:77–83.

Levkovitz Y, Roth Y, Harel EV, Braw Y, Sheer A, Zangen A (2007) A randomized controlled feasibility and safety study of deep transcranial magnetic stimulation. Clin Neurophysiol 118:2730–2744.

Levkovitz Y, et al. (2015) Efficacy and safety of deep transcranial magnetic stimulation for major depression: a prospective multicenter randomized controlled trial. World Psychiatry 14:64–73.

Li X, Lu Z, D'Argembeau A, Ng M, Bechara A (2010) The Iowa gambling task in fMRI images. Hum Brain Mapp 31:410–423.

Lin CH, Chiu YC, Cheng CM, Hsieh JC (2008) Brain maps of Iowa gambling task. BMC Neurosci 9:1.

Maresh EL, Allen JP, Coan JA (2014) Increased default mode network activity in socially anxious individuals during reward processing. Biol Mood Anxiety Disord 4:7.

McClure SM, Laibson DI, Loewenstein G, Cohen JD (2004) Separate neural systems value immediate and delayed monetary rewards. Science 306:503–507.

Moeller SJ, Gil R, Weinstein JJ, Baumvoll T, Wengler K, Fallon N, Van Snellenberg JX, Abeykoon S, Perlman G, Williams J, Manu L, Slifstein M, Cassidy CM, Martinez DM, Abi-Dargham A (2022) Deep rTMS of the insula and prefrontal cortex in smokers with schizophrenia: proof-of-concept study. Schizophrenia (Heidelb) 8:6.

O'Reardon JP, Solvason HB, Janicak PG, Sampson S, Isenberg KE, Nahas Z, McDonald WM, Avery D, Fitzgerald PB, Loo C, Demitrack MA, George MS, Sackeim HA (2007) Efficacy and safety of transcranial magnetic stimulation in the acute treatment of major depression: a multisite randomized controlled trial. Biol Psychiatry 62:1208–1216.

Park JI, Kim GW, Jeong GW, Chung GH, Yang JC (2016) Brain activation patterns associated with the effects of emotional distracters during working memory maintenance in patients with generalized anxiety disorder. Psychiatry Investig 13:152–156.

Pell GS, Roth Y, Zangen A (2011) Modulation of cortical excitability induced by repetitive transcranial magnetic stimulation: influence

of timing and geometrical parameters and underlying mechanisms. Prog Neurobiol 93:59–98.
Pizzagalli DA, Sherwood RJ, Henriques JB, Davidson RJ (2005) Frontal brain asymmetry and reward responsiveness a source-localization study. Psychol Sci 16:805–813.
Pridmore S, Fernandes Filho JA, Nahas Z, Liberatos C, George MS (1998) Motor threshold in transcranial magnetic stimulation: a comparison of a neurophysiological method and a visualization of movement method. J ECT 14:25–27.
Pu S, Nakagome K, Itakura M, Iwata M, Nagata I, Kaneko K (2016) The association between cognitive deficits and prefrontal hemodynamic responses during performance of working memory task in patients with schizophrenia. Schizophr Res 172:114–122.
Rosenberg O, Shoenfeld N, Zangen A, Kotler M, Dannon P (2010) Deep TMS in a resistant major depressive disorder: a brief report. Depress Anxiety 27:465–469.
Roth Y, Zangen A, Hallett M (2002) A coil design for transcranial magnetic stimulation of deep brain regions. J Clin Neurophysiol 19:361–370.
Roth Y, Amir A, Levkovitz Y, Zangen A (2007) Three-dimensional distribution of the electric field induced in the brain by transcranial magnetic stimulation using Figure-8 and deep H-coils. J Clin Neurophysiol 24:31–38.
Sack AT, Linden DE (2003) Combining transcranial magnetic stimulation and functional imaging in cognitive brain research: possibilities and limitations. Brain Res Brain Res Rev 43:41–56.
Siddiqi SH, Taylor SF, Cooke D, Pascual-Leone A, George MS, Fox MD (2020) Distinct symptom-specific treatment targets for circuit-based neuromodulation. Am J Psychiatry 177:435–446.
Spielberg JM, Miller GA, Warren SL, Engels AS, Crocker LD, Banich MT, Sutton BP, Heller W (2012) A brain network instantiating approach and avoidance motivation. Psychophysiology 49:1200–1214.
Stubbs RJ, Hughes DA, Johnstone AM, Rowley E, Reid C, Elia M, Stratton R, Delargy H, King N, Blundell JE (2000) The use of visual analogue scales to assess motivation to eat in human subjects: a review of their reliability and validity with an evaluation of new hand-held computerized systems for temporal tracking of appetite ratings. Br J Nutr 84:405–415.
Subramaniam K, Hooker CI, Biagianti B, Fisher M, Nagarajan S, Vinogradov S (2015) Neural signal during immediate reward anticipation in schizophrenia: relationship to real-world motivation and function. Neuroimage Clin 9:153–163.
Tendler A, Barnea Ygael N, Roth Y, Zangen A (2016) Deep transcranial magnetic stimulation (dTMS) - beyond depression. Expert Rev Med Devices 13:987–1000.
Watson D, Clark LA, Tellegen A (1988) Development and validation of brief measures of positive and negative affect: the PANAS scales. J Pers Soc Psychol 54:1063–1070.
Zhang Y, Xie B, Chen H, Li M, Liu F, Chen H (2016) Abnormal functional connectivity density in post-traumatic stress disorder. Brain Topogr 29:405–411.
Zibman S, Pell GS, Barnea-Ygael N, Roth Y, Zangen A (2021) Application of transcranial magnetic stimulation for major depression: coil design and neuroanatomical variability considerations. European Neuropsychopharmcol 45:73–88.